8-22-2020

Insights on dissolved organic matter production revealed by removal of charge-transfer interactions in senescent leaf leachates

Karl M. Meingast
Michigan Technological University, kmmeinga@mtu.edu

Brice K. Grunert
City College of New York

Sarah A. Green
Michigan Technological University, sgreen@mtu.edu

Evan S. Kane
Michigan Technological University, eskane@mtu.edu

Nastaran Khademimoshgenani
Michigan Technological University, nkhademi@mtu.edu

water

MDPI

Article

Insights on Dissolved Organic Matter Production Revealed by Removal of Charge-Transfer Interactions in Senescent Leaf Leachates

Karl M. Meingast [1,*], Brice K. Grunert [2], Sarah A. Green [3], Evan S. Kane [1,4] and Nastaran Khademimoshgenani [3]

1 College of Forest Resources and Environmental Science, Michigan Technological University, 1400 Townsend Drive, Houghton, MI 49931, USA; eskane@mtu.edu
2 City College of New York, City University of New York, 160 Convent Ave, New York, NY 10031, USA; bgrunert@ccny.cuny.edu
3 Department of Chemistry, Michigan Technological University, 1400 Townsend Drive, Houghton, MI 49931, USA; sgreen@mtu.edu (S.A.G.); nkhademi@mtu.edu (N.K.)
4 Northern Research Station, USDA Forest Service, 410 MacInnes Drive, Houghton, MI 49931, USA
* Correspondence: kmmeinga@mtu.edu

Received: 17 July 2020; Accepted: 17 August 2020; Published: 22 August 2020

Abstract: Dissolved organic matter (DOM) is a critical part of the global carbon cycle. Currently, it is understood that at least a portion of the chromophoric DOM (CDOM) character can be described through an electronic interaction of charge transfer (CT) complexes. While much work has been done to understand the influence of CT on soil and aquatic reference standard DOM, little is known about the influence of CT in fresh terrestrially derived DOM. In this study, leaf litter leachates from three tree species were treated (reduced) with sodium borohydride to determine the contribution of CT on a source of fresh terrestrial DOM. Leaf litter was sampled four times through decomposition under natural (field) conditions to determine the influence of degradation on response to borohydride treatment. Leaf litter CDOM displayed a unique loss of UVB absorption following borohydride treatment, as well as a homogenizing effect on fluorescence emission character. Humification index (HIX) differentiated Elliot Soil Humic Acid and Suwannee River Fulvic Acid from leaf litter leachates. However, biological index (BIX), and spectral slope metrics were not able to differentiate leaf leachates from these reference standards. Apparent quantum yields were similar in magnitude between leaf leachates and reference standards, although leaf leachate spectra displayed features not evident in reference standards. These results help understand the origins of DOM optical properties and associated quantitative indices in freshly sourced terrestrial material. Overall, these results suggest that even at the initial stages of decomposition, terrestrial CDOM exhibits optical characteristics and responses to removal of electron accepting ketones and aldehydes, through borohydride treatment, similar to more processed CDOM.

Keywords: charge-transfer; leaf litter; dissolved organic matter

1. Introduction

Dissolved organic matter (DOM) in freshwater systems is a complex mixture of organic molecules largely sourced from plant materials undergoing continuous biological and chemical processing across the terrestrial/aquatic interface [1]. The degree to which DOM from individual sources is processed largely determines the molecular structure and bioavailability of DOM in aquatic environments [2,3], but quantifying the processing of DOM has proven difficult [4]. Optical methods for characterization of DOM, namely absorption and fluorescence spectroscopy, offer high throughput and detailed

characterization of the chromophoric DOM (CDOM) in aquatic environments [5–7]. However, there are still unresolved interactions among seemingly unique CDOM components [4] which make linkages of distinct chromophores to molecular structures difficult [5–7].

Intramolecular electronic interactions (EI), defined as charge transfer (CT) interactions, has been proposed as a model to explain the distinct exponential loss of absorption with increasing wavelength in CDOM [8]. Recent studies probing origins of aquatic DOM under the premise of the EI model have employed reduction of natural samples with sodium borohydride. Sodium borohydride causes selective reduction of carbonyl containing ketones and aldehydes, removing the electron acceptors of CT interactions [9–16]. The effects of borohydride treatment on the CDOM optical properties are two-fold: (i) the removal of CT interactions through the reduction of select electron acceptors decreases absorbance, and (ii) increases fluorescence by electron donors that are no longer quenched by CT relaxation pathways [13]. Electron accepting moieties responsible for CT also play an important role in the ability of DOM to act as a terminal electron acceptor during anaerobic respiration in aquatic environments [17,18].

A bulk of the work probing the importance of CT has been centered in aquatic environments which represent "downstream" environments of CDOM originating from terrestrial sources that has undergone various degrees of humification. For example, Suwannee River Fulvic Acid (SRFA), which is often used as a terrestrial reference material [10,12,14], originates from a collection point at the Suwanee River's headwaters, and represents a highly degraded DOM pool, which has likely undergone much microbial, and some photochemical processing, compared to terrestrial vegetation inputs [19]. The terrestrial/aquatic interface "upstream" of where SRFA is collected has been shown to be a hotspot in DOM processing [20]. Therefore, we hypothesize that fresh terrestrial DOM, yet to reach this interface, and containing relatively high concentrations of ketones and aldehydes in partially oxidized phenolic moieties, may display a greater sensitivity to CT reductions. This sensitivity is likely caused by the prevalence of electron accepting carbonyl moieties, as well as presumed donors such as polyphenols and substituted aromatic carboxylic acids in relatively unprocessed DOM [21].

Fundamental differences in photochemical properties between aquatic and soil reference substances have been demonstrated using reference standards from the International Humic Substances Society (IHSS) [22]. As such, SRFA has been used as an aquatic reference and Elliot Soil Humic Acid (ESHA) as a soil reference [22]. This work has suggested three main differences in electrochemical and photochemical properties between DOM in terrestrial (e.g., soil) and aquatic environments:

(1) Soil HA displayed higher electron accepting capacity (EAC) and lower electron donating capacity (EDC) than aquatic DOM.
(2) Lower wavelength absorption tracked changes in EAC in soil HA, to a greater degree than aquatic DOM.
(3) Lower wavelength absorption appeared to track EDC during photodegradation of aquatic DOM, indicating that this absorption is influenced by oxidative removal of electron donors, such as phenols, more in aquatic environments than in soils.

The mechanism behind these findings is unclear because electron donors, such as low molecular weight phenolics, are likely delivered from the terrestrial environment, and therefore would be expected to contribute more in upstream (e.g., soil) than further downstream (e.g., aquatic) environments. Similar humic-like features have been observed in degradation of lignin-free phytoplankton DOM [14], suggesting that the humic-like fluorescence character is not exclusive to lignin derivatives acting as terrestrially-derived electron donors. Rather, it appears that microbial processing transfers the initial optical properties of source material, along with a modified humic-like signal that can significantly contribute to CT interactions in the produced DOM. In this way, the attribution of optical properties to a particular source can be confused by ubiquitous microbial fingerprints superimposed across terrestrial and aquatic environments [23].

Understanding CT interactions in natural waters warrants an understanding of the source of DOM and the role of microbes in altering its signal, particularly for understanding processes that

span the terrestrial/aquatic interface. The main DOM inputs to both soils and aquatic environments in forested ecosystems are from groundwater and precipitation mediated leaching of plant materials, or throughfall [20]. Much of the leachable DOM is removed from leaves during the autumn season [24,25]. In forested watersheds, DOM leached by throughfall is stored in soils, and some is transported directly to the aquatic environment by leaf litter falling into the stream channel [26]. Regardless of its fate, freshly fallen leaf litter represents one of the youngest and most constant pulses of terrestrial CDOM delivered to aquatic environments from the terrestrial environment.

This study investigated CT influence on optical properties of leaf litter (O_i soil horizon) leachates from three different tree species collected in situ spanning a time frame from directly after leaf fall to the following spring. We compared the CT influence in leaf leachates to CT characteristics in soil and aquatic reference standards to accurately characterize a source of fresh terrestrial DOM and the associated early stages of decomposition to both soil and aquatic, terrestrially sourced, ecosystems. The main aim of this study was to optically characterize young, terrestrially sourced DOM and observe how degradation modifies the source DOM composition, as observed through CT interactions.

2. Materials and Methods

2.1. Experimental Design

Leaf leachates were made from three species, Sugar maple (*Acer saccharum* Marsh), Paper birch (*Betula papyrifera* Marsh), and Red oak (*Quercus rubra* L.), herein referred to as maple, birch, and oak, respectively. A total of 10 g of leaves from each species were randomly collected from unmanipulated plots adjacent to the USDA Forest Service Rhizotron Facility in Houghton, MI (https://www.nrs.fs.fed.us/research/facilities/rhizotron/). To assess changes in leaf leachates with biological processing, we harvested leaves on four occasions, from November to June. For each experiment, 5.0 g of homogenized fresh leaves cut into 2.5 cm^2 sections were soaked in 250 mL MilliQ water for 4 h, (similar to [25]). Leaf leachates were then vacuum filtered through 0.7 µm GF/F filters followed by 0.45 µm nylon filters and added to 500 mL pre-combusted glass bottles. Samples were stored in the dark at 4 °C, to minimize additional microbial processing after extraction.

Reference standards SRFA and ESHA were chosen as representative aquatic and soil reference materials and to compare our results with recent studies [4,8]. 5.0 mg of SRFA and 2.0 mg of ESHA were solubilized overnight in 100 mL MilliQ water adjusted using high purity NaOH (Fisher) to pH 9. These stock solutions were then adjusted to pH 7 and diluted with MilliQ to desired concentrations. Absorption and fluorescence spectra were measured for SRFA and ESHA at 25.0 mg L^{-1} and 6.7 mg L^{-1} respectively, which gave an absorbance of 0.6 at excitation 250 nm.

2.2. Optical Measurements

Absorption and fluorescence spectra were measured on a Horiba Aqualog in a 1 cm quartz cell (Starna Cells, Inc., Atascadero, CA, USA). Absorption spectra were run from 240 nm to 800 nm at 1 nm resolution. Leachates were diluted to ensure measurements fell into the linear range of the instrument if necessary. Fluorescence spectra were recorded at 1 nm excitation wavelengths from 240 to 800 nm, and emission was recorded at 3 nm resolution from 240 to 640 nm. Fluorescence spectra were converted to Raman units using Raman scattering from a sealed MilliQ cuvette (Starna) (R.U.) and quinine sulfate equivalents (Q.S.E.) using the fluorescence at 350 nm (ex 350, em 290–600) of 10 ppb quinine sulfate (NIST) in 0.105 M $HClO_4$ (VWR). Absorbance values were converted to Naperian absorption coefficients (a_λ) [27]:

$$a_\lambda = 2.303\frac{A_\lambda}{L} \quad (1)$$

where L is the pathlength, in meters and A_λ is wavelength specific absorbance. Absorption spectra were blank subtracted with MilliQ for untreated spectra and a procedural blank for borohydride treated samples. All measurements were taken at pH 7. Inner filter effects, Raman scattering, and Raleigh scattering for fluorescence EEMs were removed using the PLS toolbox (v782; Eigenvector) in Matlab

(2014a) (The MathWorks Inc., Natick, MA, USA). Derived parameters from absorption spectra were E2:E3 and spectral slopes. E2:E3 was defined as:

$$\text{E2 : E3} = \frac{a_{250}}{a_{365}}, \tag{2}$$

where a_{250} is absorption at 250 nm and a_{365} is absorption at 365 nm.

$S_{275–295}$ and $S_{350–400}$ values were calculated as the slopes of linear regressions of log-transformed absorption spectra from 275–295 nm and 350–400 nm respectively [7].

Derived parameters from the fluorescence spectra were the biological index (BIX) [28] and humification index (HIX) [29,30] and were defined as:

$$\text{BIX} = \frac{F_{380}}{F_{430}}, \tag{3}$$

where F_{380} and F_{430} are emission at 380 nm and 430 nm, respectively, for excitation at 310 nm.

$$\text{HIX} = \frac{\Sigma F_{435–480}}{\Sigma F_{300–345}}, \tag{4}$$

where ΣF is the integrated emission over the indicated wavelength ranges for excitation 255 nm.

Absorption changes following borohydride treatment are reported as:

$$\frac{\Delta a}{a} = \frac{a(0) - a(t)}{a(0)}, \tag{5}$$

where $a(0)$ is absorption before borohydride treatment and $a(t)$ is absorption after borohydride treatment.

Apparent quantum yields (Φ_{app}) were calculated at each excitation wavelength from 240 to 600 nm, relative to a 10 ppb solution of quinine sulfate [27]:

$$\Phi_{app} = 0.60 \left(\frac{I_{s,\lambda}}{I_{QS,350}} \times \frac{a_{QS,350}}{a_{s,\lambda}} \right), \tag{6}$$

where 0.60 accounts for 10 ppb quinine sulfate in 0.105 M perchloric acid [31]. $I_{s,\lambda}$ is the integrated sample fluorescence emission intensity at the excitation wavelength (λ). $I_{QS,350}$ is the fluorescence emission intensity of quinine sulfate at excitation 350 nm. $a_{QS,350}$ is the absorption coefficient of quinine sulfate at excitation 350 nm and $a_{s,\lambda}$ is the integrated sample absorption coefficient the excitation wavelength.

2.3. Borohydride Treatments

Leaf leachates were adjusted to pH 7 and pH 10 using high purity NaOH (Fisher, Hampton, NH, USA), and the optical properties were recorded for each pH. A total of 17.0 mg of sodium borohydride (Acros Organics, Hampton, NH, USA) was added to 17.0 mL of leaf tea, and the reactions were allowed to proceed for 48 h [16]. Leachates were then filtered through 0.45 µm nylon filters and optical properties were again recorded at pH 10, pH 7 and natural pH. Additions of $HClO_4$ were used to adjust pH (VWR). Results are reported at a neutral pH of 7, as recommended by [16]. All experiments were run with three analytical replicates. Under visual inspection, some experiments displayed unique variation in absorption spectral shape for individual replicates before treatment. To ensure representativeness, the average of the two most similar experimental replicates was reported for all experiments (see also, NASA optical measurement protocol; [32]).

3. Results

3.1. Absorption Change after Borohydride Treatments

Following borohydride treatment, all leaf leachates at all time points displayed a loss of absorption in the UV (particularly the UVB (280–315 nm)). The normalized difference spectra (Figure 1) show that approximately 20–60% of the original absorption was lost from 250–400 nm, generally increasing with

wavelength. Longer wavelength loss was similar for all three of the autumn samples. The spring samples (May 2019) displayed a smaller loss in absorption from the borohydride treatment. Those samples had significantly lower absorption at wavelengths greater than 400 nm (Figure S1). The magnitude of this loss for IHSS reference standards was similar to that of birch and maple. Oak showed a greater fraction of absorption loss than IHSS standards, consistently displaying the highest absorption loss of the leachates (Figure 1). A key feature, a peak around 280 nm, became more pronounced after borohydride treatment for all leaf leachates (Figure S1). Spectral changes between species and among the autumn samples were not as large as the changes from December to May (Figure 1).

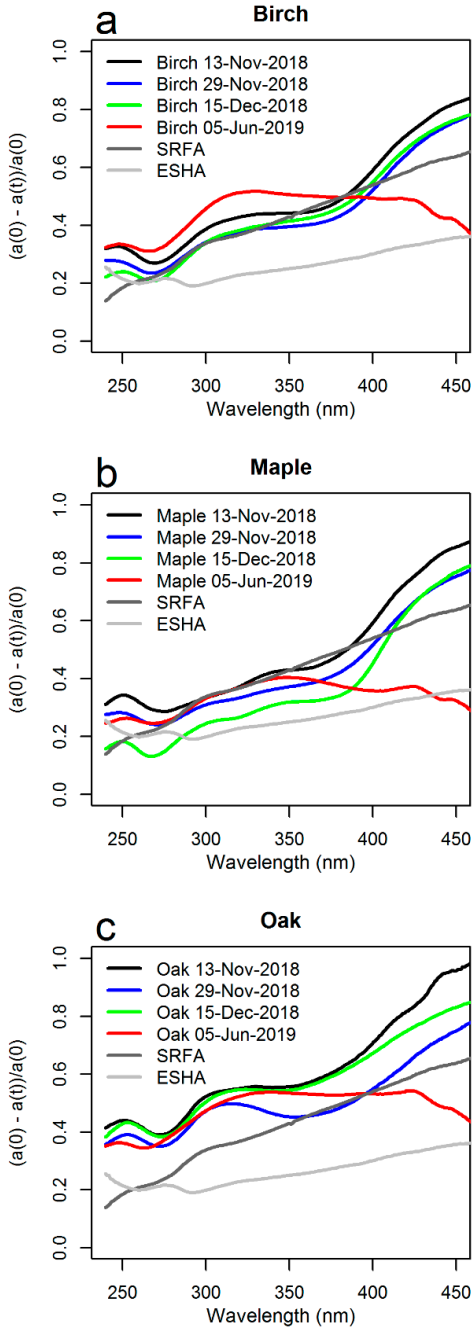

Figure 1. Change in absorption following borohydride treatment for (**a**) birch leachates, (**b**) maple leachates, and (**c**) oak leachates. All leaf litter leachates, excluding maple 15 December 2018 displayed higher loss of UV absorption following treatment. Additionally, the litter from June 2019 all displayed decreased response to borohydride from 400–500 nm in relation to the autumn leachates and reference standards.

Oak DOM showed a greater sensitivity to borohydride treatment than birch and maple. Oak and birch displayed two broad regions of absorption that were less impacted by borohydride treatment, centered around 280 and 370 nm, suggesting the presence of unaltered chromophore groups in these spectral regions. For CDOM only participating in charge-transfer, spectra in Figure 1 should present a monotonic increase from shorter to longer wavelengths, representing the increasing contribution of CT to total absorption at longer wavelengths.

For all leaf leachates, there is a consistent decrease in response to borohydride treatment from 13 November 2018 to 29 November 2018. Maple continues to display a decrease from 29 November 2018 to 15 December 2018, while birch and oak show an increase. All leaf leachates displayed an increasing response from 15 December 2018 to 5 June 2019, with birch showing a greater response to borohydride treatment at 6 May 2019 than in the initial sample from 13 November 2018.

When spectra are characterized as $S_{350–400}$ and $S_{275–295}$, leaf leachate absorption is within the range of reference standards and therefore not easily distinguished, even following borohydride treatment (Figure 2). Both $S_{350–400}$ and $S_{275–295}$ increased for each species following borohydride treatment, similar to SRFA. However, the range of oak leachates overlapped with the borohydride treated maple and birch leachates.

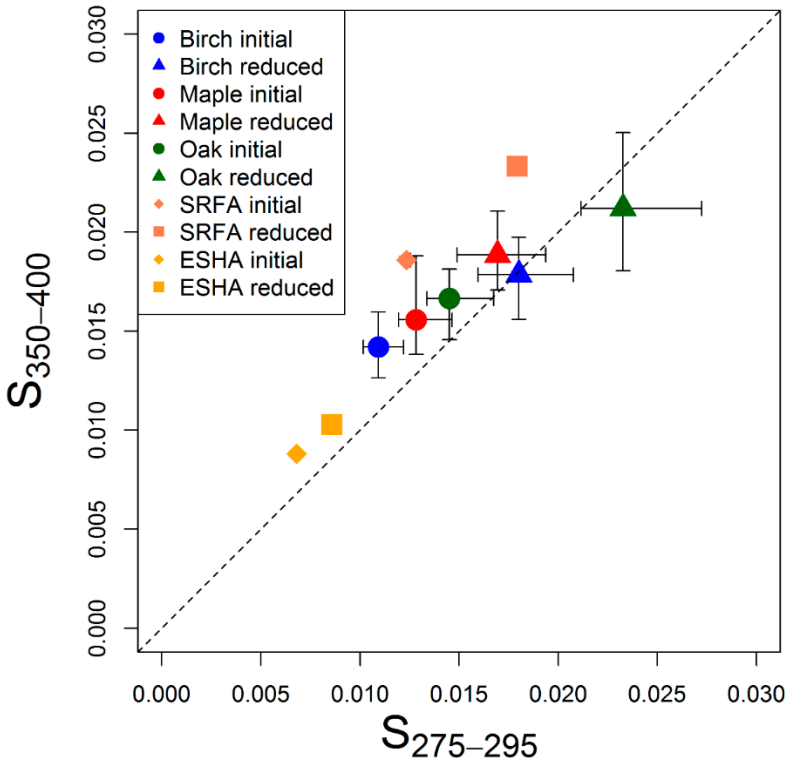

Figure 2. Mean absorption indices, $S_{275–295}$ and $S_{350–400,}$ for leaf litter leachates. Borohydride treatment (reduced) causes increases in both metrics for all samples. Both spectral slopes do not appear to distinguish leaf leachates from HA and FA standards. Error bars indicate range of values for all four time points of each species. Dashed line indicates a spectral ratio of 1.

3.2. Fluorescence Response to Borohydride Treatment

Fluorescence response to borohydride is best represented through Φ_{app} spectra [27]. Magnitudes of Φ_{app} of all treated and untreated samples were similar to IHSS reference standards (Figure 3). The most evident defining characteristics in contrast to IHSS reference standards was the emergence of two local maxima between 300–400 nm following borohydride treatment (Figure 3). Oak was least changed through time (Figure 3). The leachates collected 5 June 2019 displayed less structure than

the earlier times as well as no increase in Φ_{app} in response to borohydride treatment at greater than 500 nm (Figure 3).

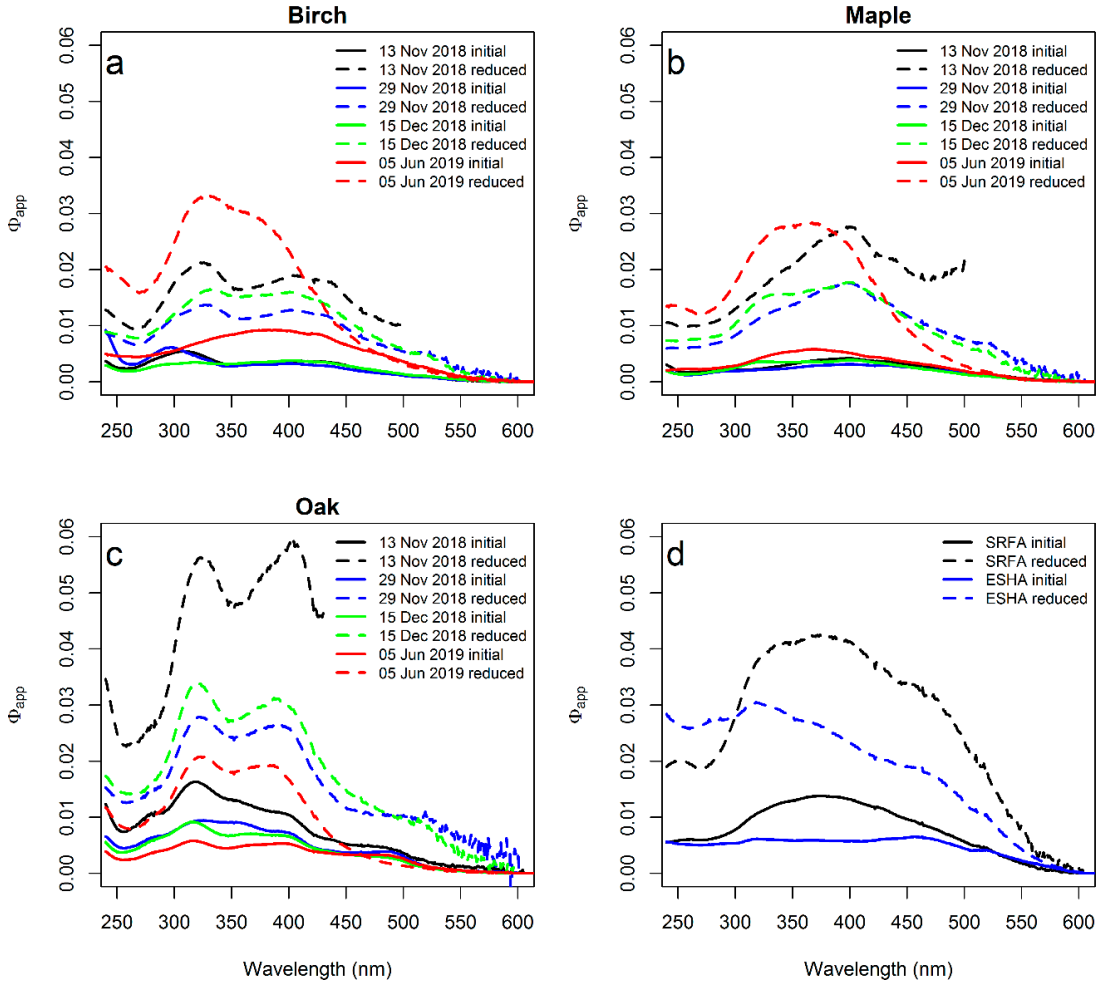

Figure 3. Apparent quantum yield (Φ_{app}) before and after borohydride treatment (reduced) for (**a**) birch leachates, (**b**) maple leachates, (**c**) oak leachates, and (**d**) International Humic Substances Society (IHSS) reference standards. Maple leachates showed lowest Φ_{app}. By 5 June 2019, all leachates had converged on similar spectra except for oak which preserved three distinct peaks in the Φ_{app} spectrum through 7 months of degradation. Although Φ_{app} were variable through time, there is no evident trend in the magnitude.

When fluorescence was characterized as BIX, leaf leachate CDOM absorption was within the range of the reference standards, and is therefore not easily distinguished. On the other hand, HIX displayed separation between IHSS reference standards and leaf litter leachates (Figure 4). BIX increased in all species following borohydride treatment, yet HIX was unresponsive for Oak. SRFA displayed a unique decreasing response in HIX, following borohydride treatment. This response was not observed in leaf litter leachates or ESHA.

HIX increased through time in maple and oak leachates. Birch leachates also increased in HIX although there was a slight decrease between the first two time points (Table 1). BIX did not change through time.

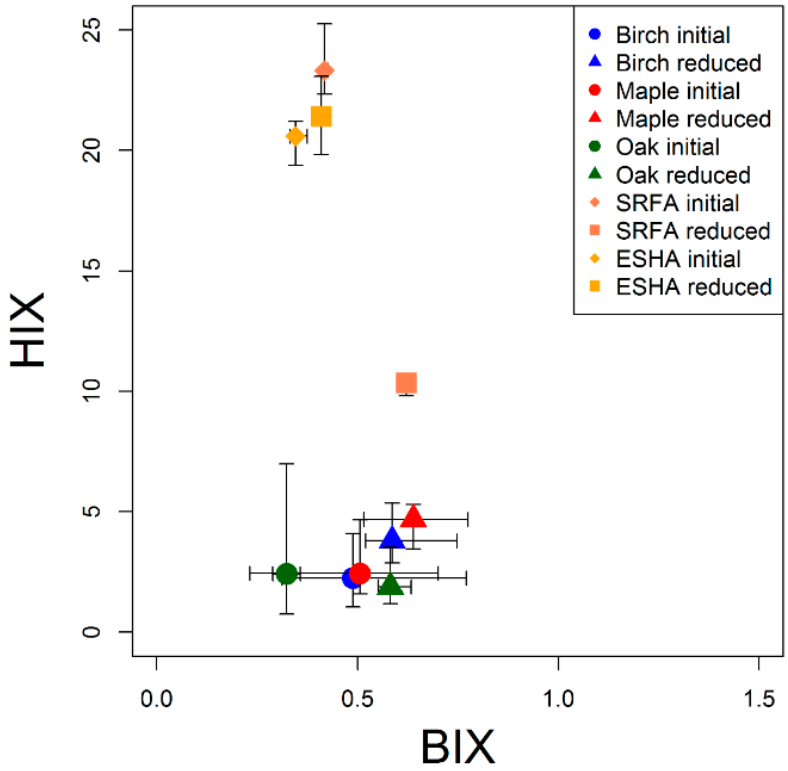

Figure 4. Mean, biological index (BIX), and humification index (HIX) for leaf litter leachates. Leaf litter and planktonic chromophoric dissolved organic matter (CDOM) exhibit low HIX, but slightly different BIX (BIX characterizes shape of emission at 310 nm excitation. HIX characterizes shape of emission at 255 excitation). Suwannee River Fulvic Acid (SRFA) decrease in HIX following treatment is not observed in other samples, including Elliot Soil Humic Acid (ESHA). Error bars represent the range of values for all four time points for each species.

Table 1. Optical and chemical metrics of leaf leachates and reference materials. Graphically displayed in figures.

	pH	DOC (mg L^{-1})	E2:E3	BIX	HIX	$S_{275–295}$	$S_{350–400}$
13 November 2018							
Birch initial	6.1	20.7	3.6	0.3	1.4	0.010	0.014
Birch reduced			4.4	0.5	2.9	0.017	0.020
Maple initial	5.2	11.1	3.9	0.7	1.6	0.012	0.015
Maple reduced			4.6	0.8	3.4	0.015	0.021
Oak initial	6.2	17.6	5.2	0.3	0.7	0.017	0.017
Oak reduced			6.9	0.6	1.2	0.027	0.025
29 November 2018							
Birch initial	6.0	11.0	3.4	0.8	1.0	0.010	0.014
Birch reduced			4.1	0.5	3.9	0.016	0.019
Maple initial	5.6	14.3	3.6	0.6	1.7	0.012	0.015
Maple reduced			4.3	0.6	5.3	0.015	0.020
Oak initial	6.1	20.6	4.8	0.4	0.9	0.014	0.017
Oak reduced			5.4	0.6	1.3	0.023	0.021
15 December 2018							
Birch initial	6.1	20.6	3.2	0.4	2.5	0.011	0.013
Birch reduced			4.2	0.5	5.4	0.018	0.018
Maple initial	4.8	14.0	3.3	0.2	1.8	0.013	0.014
Maple reduced			4.0	0.5	5.2	0.018	0.017
Oak initial	6.5	15.2	4.4	0.3	1.0	0.013	0.015
Oak reduced			5.8	0.6	1.5	0.022	0.021

Table 1. *Cont.*

	pH	DOC (mg L^{-1})	E2:E3	BIX	HIX	$S_{275–295}$	$S_{350–400}$
5 June 2019							
Birch initial	6.8	12.5	4.0	0.5	4.1	0.012	0.016
Birch reduced			5.3	0.7	3.0	0.021	0.016
Maple initial	6.1	17.6	4.0	0.5	4.7	0.015	0.019
Maple reduced			4.9	0.6	4.8	0.019	0.017
Oak initial	6.1	20.7	4.7	0.4	7.0	0.014	0.018
Oak reduced			6.4	0.6	3.5	0.021	0.018
References							
SRFA initial	–	10.2	4.6	0.4	23.3	0.012	0.019
SRFA reduced			6.8	0.6	10.3	0.018	0.023
ESHA initial	–	3.2	2.3	0.6	1.5	0.007	0.009
ESHA reduced			2.8	0.5	5.4	0.009	0.010

4. Discussion

Following borohydride treatment, carbonyls, specifically ketones and aldehydes, are removed from DOM [13]. As these chromophoric moieties are converted to colorless alcohols, absorption decreases. Additionally, borohydride likely removes electron transfer pathways that quench fluorescence, thereby increasing fluorescence intensities. Plant tissues such as lignin derivatives, higher in carbonyls than lignin itself, are therefore expected to exhibit a significant response to borohydride treatment. The findings presented herein are in support of this hypothesis.

4.1. Absorption Response to Borohydride

Absorption decreased in all leaf leachates following borohydride treatment. Shorter wavelength absorption (UVB) decreased in autumn leaf litter more than SRFA and ESHA (Figure 1). This supports the findings of [4], that electron acceptors play a larger role in UVB absorption in fresh relative to aged CDOM. Interestingly, unlike leaf litter leachates, fresh planktonic DOM does not exhibit decreases in UVB absorption following borohydride treatment [14]. This supports the hypothesis that partially oxidized products of degradation play an important role as CT donors in increasingly fresh terrestrial DOM, as these moieties are expected to be present and contribute significantly in leaf litter; such degradation products may not be present in phytoplankton derived DOM.

Changes in the visible region due to borohydride treatment of the autumn leachates were consistent with soil and aquatic HA (Figure 1, Figure S1). However, the most evident change in leaf leachate absorption through time occurred in leachates from leaves that had aged under the snow over the winter. These samples showed a loss of the longer wavelength response to borohydride which was dramatically different from SRFA and ESHA (Figures 1 and 2). This loss extends the findings of Sharpless and Blough [4], by showing the sensitivity of fresh terrestrial CDOM to removal of electron acceptors following borohydride treatment. However, it is unclear why the earlier leaf leachates tracked reference standards better than the more aged leaf matter. More aged DOM that is more condensed (lower H:C) and/or more aromatic should result in higher electron accepting capacity [33,34]. One hypothesis is that these electron acceptors, with relatively high quinone contents [13], are preferentially removed through leaching during snowmelt, due to their higher molecular weight. Interestingly, the higher UVB absorption losses are conserved into the spring for all leachates. This suggests that UVB absorption response to borohydride may not be an indicator of DOM processing, but rather a descriptor of source, and is further supported by the unique increase in UVB absorption of phytoplankton derived DOM to borohydride treatment [14].

E2:E3, $S_{275–295}$, and $S_{350–400}$ all increased following borohydride treatment (Table 1). These increases contrast fresh and degraded phytoplankton DOM, which was reported to decrease in spectral slope following borohydride treatment [14]. This significant deviation between algal and terrestrial DOM

inputs is likely driven by the absorption peak observed around 350 nm. These findings highlight the utility of E2:E3 as a robust indicator of EAC, even in terrestrial materials [17,22]. $S_{275–295}$ did not appear to differentiate leaf litter leachates from IHSS reference standards. Furthermore, $S_{275–295}$ increased following borohydride treatment, displaying its sensitivity to processes other than changes in DOM molecular weight, for which it is often employed. Overall, absorption characteristics changed in response to borohydride treatment, indicating that the metrics reported here may not be independent of DOM processing, and therefore are not recommended to infer DOM source.

4.2. Fluorescence Response to Borohydride

The fluorescence of leaf leachates showed multiple features in the Φ_{app} spectra with considerable variability between samples producing more structured Φ_{app} spectra in leaf leachates than SRFA and ESHA (Figure 3). Specifically, the leaf leachates generally displayed two unique maxima between 300–400 nm following borohydride treatment. An important note is that these maxima appear to be blue shifted or red shifted from the original spectra depending on sample. These findings suggest that the initial maxima may not be directly related to the maxima of the borohydride treated sample (e.g., blue shifting of a fluorophore's peak fluorescence), even though they exhibit similar spectral signatures.

Multiple insights can be gained simply through the interpretation of leaf leachate fluorescence as HIX and BIX. For one, leaf leachates display lower HIX than reference standards, and are similar to planktonic CDOM, presumably indicating similar amounts of conjugation between these source materials. Contrarily, BIX does not differentiate leaf leachates from either SRFA or ESHA, however, leaf leachates appear to exhibit lower BIX than planktonic CDOM [14]. Interestingly, all of these patterns are preserved following borohydride treatment, indicating the uniqueness of each source's fluorescent character when represented as HIX and BIX. However, HIX and BIX did not differentiate between species of leaf leachates.

Another interesting finding is the removal of the fluorescent peak at (excitation 280 nm/emission 350 nm), often referred to as tryptophan-like, following borohydride treatment. This change is most evident in the 29 November 2018 Birch leachate (Figure S2). The occurrence of this peak only in select leachates suggests that this peak is an intermediate product of DOM processing, consistent with [19]. In addition, this peak can be removed when treated by borohydride (Figure S2). Pearl et al. [35] showed that relatively minor modifications to small molecules exhibiting protein-like fluorescence can dramatically shift the observed fluorescence signal. The peak observed here (excitation 280 nm/emission 350 nm) exhibits tryptophan-like fluorescence, yet is removed by borohydride treatment, which would not be expected for tryptophan. This suggests that the tryptophan-like fluorescence observed here is produced by partially oxidized organic compounds, which exhibit protein-like fluorescence (perhaps catechins [36]), yet becomes less fluorescent or emission shifted in response to borohydride treatment. Murphy et al. [37] observed a similar tryptophan-like fluorescent feature in pharmaceutically derived sodium salicylate, providing strong evidence for compounds other than proteins to produce protein-like fluorescence. Our results provide additional evidence that forest-derived phenolics may be responsible for this fluorescent feature in many aquatic environments. Further work employing a combination of mass spectroscopy with borohydride treatment is warranted, to understand the unique molecules contributing to this fluorescent feature.

4.3. Tree Species Differences

The variation in borohydride response through time outweighs species differences between birch and maple in both absorption and fluorescence efficiencies (Figures 1 and 3), suggesting that microbial and fungal degradation of leaf litter can manifest into a common optical signature from a variety of terrestrial source material. This is consistent with recent work suggesting a homogenization of source signals into a complex, non-unique signal in aquatic DOM, largely attributed to photo- and microbial transformations of source material [23]. Oak displays a much more structured Φ_{app} spectra compared to the other species and is more consistently changed over time (Figure 3). Oak leaf chemistry is known

to inhibit decomposition [38], and therefore, our results are likely tracking a prolonged process of decomposition not captured for the other species, with a reduced microbial and fungal decomposition signal. However, at 5 June 2019, all three species had lost the long wavelength absorption, responsive to borohydride treatment, found in the previous time points and present in SRFA and ESHA. The longer wavelength absorption is stable through the autumn, so this absorption may represent a recalcitrant fraction of fresh DOM, removed from leaf litter by leaching.

5. Conclusions

Our findings displayed an overall similar response of fresh leaf litter leachates and IHSS reference standards to borohydride treatment, with largely similar percentages of absorption loss as well as fluorescence gained among samples following borohydride treatment. However, our findings highlight the complex and highly variable signatures associated with a fresh terrestrial DOM among deciduous broadleaf tree species and through time, even following borohydride treatment. Further work is warranted to understand if these responses are consistent for coniferous tree species, as well as woody and herbaceous shrubs. Although HIX was able to differentiate IHSS standards from leaf leachates both before and after borohydride treatment, we stress the variability of end-member signatures, even after removal of the CT "haziness", which make inferences to DOM source not recommended. These results confirm that absorption and fluorescence indices from fresh DOM sources—particularly protein-like fluorescence—are sensitive to redox environment, and therefore redox conditions need to be considered when comparing optical data from different electrochemical environments.

Supplementary Materials: The following are available online at http://www.mdpi.com/2073-4441/12/9/2356/s1, Figure S1: Absorption spectra from leaf leachates and reference standards, before (black) and after (red) borohydride treatments. Most notably, the higher loss of absorption in the 250–280 nm range. Figure S2: Excitation Emission matrices (EEMs) from three different species of leaf leachates collected on three different dates through autumn 2018 and once in spring 2019. Intensities are reported in Raman Units (R.U.).

Author Contributions: Conceptualization, K.M.M., B.K.G. and E.S.K.; Data curation, K.M.M.; Formal analysis, K.M.M., B.K.G., S.A.G. and E.S.K.; Funding acquisition, K.M.M. and E.S.K.; Investigation, K.M.M. and N.K.; Methodology, K.M.M. and B.K.G.; Resources, E.S.K.; Supervision, E.S.K.; Visualization, B.K.G., S.A.G. and E.S.K.; Writing—original draft, K.M.M., B.K.G. and E.S.K.; Writing—review & editing, K.M.M., B.K.G., S.A.G., E.S.K. and N.K. All authors have read and agreed to the published version of the manuscript.

Funding: This research was funded by a NASA Earth and Space Sciences Fellowship, grant number NNX16AN96H

Acknowledgments: The authors would like to thank Tim Veverica for the helpful discussions and assistance with the methodology. We would also like to thank Carmen Cartisano for guidance on borohydride treatment methodology. We would also like to thank Amy Marcarelli, Lynn Mazzolini and Amna Ijaz Mahmud for DOM reading group discussions helping synthesize the literature.

Conflicts of Interest: The authors declare no conflict of interest.

References

1. Fisher, S.G.; Likens, G.E. Energy flow in Bear Brook, New Hampshire: An integrative approach to stream ecosystem metabolism. *Ecol. Monogr.* **1973**, *43*, 421–439. [CrossRef]
2. Fellman, J.B.; Hood, E.; D'amore, D.V.; Edwards, R.T.; White, D. Seasonal changes in the chemical quality and biodegradability of dissolved organic matter exported from soils to streams in coastal temperate rainforest watersheds. *Biogeochemistry* **2009**, *95*, 277–293. [CrossRef]
3. Inamdar, S.; Dhillon, G.; Singh, S.; Dutta, S.; Levia, D.; Scott, D.; McHale, P. Temporal variation in end-member chemistry and its influence on runoff mixing patterns in a forested, Piedmont catchment. *Water Resour. Res.* **2013**, *49*, 1828–1844. [CrossRef]
4. Sharpless, C.M.; Blough, N.V. The importance of charge-transfer interactions in determining chromophoric dissolved organic matter (CDOM) optical and photochemical properties. *Environ. Sci. Process. Impacts* **2014**, *16*, 654–671. [CrossRef]
5. McKnight, D.M.; Boyer, E.W.; Westerhoff, P.K.; Doran, P.T.; Kulbe, T.; Andersen, D.T. Spectrofluorometric characterization of dissolved organic matter for indication of precursor organic material and aromaticity. *Limnol. Oceanogr.* **2001**, *46*, 38–48. [CrossRef]

6. Weishaar, J.L.; Aiken, G.R.; Bergamaschi, B.A.; Fram, M.S.; Fujii, R.; Mopper, K. Evaluation of specific ultraviolet absorbance as an indicator of the chemical composition and reactivity of dissolved organic carbon. *Environ. Sci. Technol.* **2003**, *37*, 4702–4708. [CrossRef]
7. Helms, J.R.; Stubbins, A.; Ritchie, J.D.; Minor, E.C.; Kieber, D.J.; Mopper, K. Absorption spectral slopes and slope ratios as indicators of molecular weight, source, and photobleaching of chromophoric dissolved organic matter. *Limnol. Oceanogr.* **2008**, *53*, 955–969. [CrossRef]
8. Del Vecchio, R.; Blough, N.V. On the origin of the optical properties of humic substances. *Environ. Sci. Technol.* **2004**, *38*, 3885–3891. [CrossRef]
9. Ma, J.; Del Vecchio, R.; Golanoski, K.S.; Boyle, E.S.; Blough, N.V. Optical properties of humic substances and CDOM: Effects of borohydride reduction. *Environ. Sci. Technol.* **2010**, *44*, 5395–5402. [CrossRef]
10. Andrew, A.A.; Del Vecchio, R.; Subramaniam, A.; Blough, N.V. Chromophoric dissolved organic matter (CDOM) in the Equatorial Atlantic Ocean: Optical properties and their relation to CDOM structure and source. *Mar. Chem.* **2013**, *148*, 33–43. [CrossRef]
11. Andrew, A.A.; Del Vecchio, R.; Zhang, Y.; Subramaniam, A.; Blough, N.V. Are extracted materials truly representative of original samples? Impact of C18 extraction on CDOM optical and chemical properties. *Front. Chem.* **2016**, *4*, 4. [CrossRef]
12. Cartisano, C.M.; Del Vecchio, R.; Bianca, M.R.; Blough, N.V. Investigating the sources and structure of chromophoric dissolved organic matter (CDOM) in the North Pacific Ocean (NPO) utilizing optical spectroscopy combined with solid phase extraction and borohydride reduction. *Mar. Chem.* **2018**, *204*, 20–35. [CrossRef]
13. Del Vecchio, R.; Schendorf, T.M.; Blough, N.V. Contribution of quinones and ketones/aldehydes to the optical properties of humic substances (HS) and chromophoric dissolved organic matter (CDOM). *Environ. Sci. Technol.* **2017**, *51*, 13624–13632. [CrossRef]
14. Osburn, C.L.; Kinsey, J.D.; Bianchi, T.S.; Shields, M.R. Formation of planktonic chromophoric dissolved organic matter in the ocean. *Mar. Chem.* **2019**, *209*, 1–13. [CrossRef]
15. Schendorf, T.M.; Del Vecchio, R.; Bianca, M.; Blough, N.V. Combined effects of pH and borohydride reduction on optical properties of humic substances (HS): A comparison of optical models. *Environ. Sci. Technol.* **2019**, *53*, 6310–6319. [CrossRef]
16. Schendorf, T.M.; Del Vecchio, R.; Koech, K.; Blough, N.V. A standard protocol for NaBH4 reduction of CDOM and HS. *Limnol. Oceanogr. Methods* **2016**, *14*, 414–423. [CrossRef]
17. Kane, E.S.; Veverica, T.J.; Tfaily, M.M.; Lilleskov, E.A.; Meingast, K.M.; Kolka, R.K.; Chimner, R.A. Reduction-oxidation potential and dissolved organic matter composition in Northern Peat Soil: Interactive controls of water table position and plant functional groups. *J. Geophys. Res. Biogeosci.* **2019**, *124*. [CrossRef]
18. Walpen, N.; Getzinger, G.J.; Schroth, M.H.; Sander, M. Electron-donating phenolic and electron-accepting quinone moieties in peat dissolved organic matter: Quantities and redox transformations in the context of peat biogeochemistry. *Environ. Sci. Technol.* **2018**, *52*, 5236–5245. [CrossRef]
19. D'Andrilli, J.; Junker, J.R.; Smith, H.J.; Scholl, E.A.; Foreman, C.M. DOM composition alters ecosystem function during microbial processing of isolated sources. *Biogeochemistry* **2019**, *142*, 281–298. [CrossRef]
20. Wantzen, K.M.; Junk, W.J. Aquatic-terrestrial linkages from streams to rivers: Biotic hot spots and hot moments. *Arch. Hydrobiol. Suppl.* **2006**, *16*, 595–611. [CrossRef]
21. Qualls, R.G.; Haines, B.L. Geochemistry of dissolved organic nutrients in water percolating through a forest ecosystem. *Soil Sci. Soc. J.* **1991**, *55*, 1112–1123. [CrossRef]
22. Sharpless, C.M.; Aeschbacher, M.; Page, S.E.; Wenk, J.; Sander, M.; McNeill, K. Photooxidation-induced changes in optical, electrochemical, and photochemical properties of humic substances. *Environ. Sci. Technol.* **2014**, *48*, 2688–2696. [CrossRef]
23. Harfmann, J.L.; Guillemette, F.; Kaiser, K.; Spencer, R.G.; Chuang, C.Y.; Hernes, P.J. Convergence of terrestrial dissolved organic matter composition and the role of microbial buffering in aquatic ecosystems. *J. Geophys. Res. Biogeosci.* **2019**, *124*, 3125–3142. [CrossRef]
24. McDowell, W.H.; Fisher, S.G. Autumnal processing of dissolved organic matter in a small woodland stream ecosystem. *Ecology* **1976**, *57*, 561–569. [CrossRef]
25. McKnight, D.M.; Smith, R.L.; Harnish, R.A.; Miller, C.L.; Bencala, K.E. Seasonal relationships between planktonic microorganisms and dissolved organic material in an alpine stream. *Biogeochemistry* **1993**, *21*, 39–59. [CrossRef]

26. Meyer, J.L.; Wallace, J.B.; Eggert, S.L. Leaf litter as a source of dissolved organic carbon in streams. *Ecosystems* **1998**, *1*, 240–249. [CrossRef]
27. Green, S.A.; Blough, N.V. Optical absorption and fluorescence properties of chromophoric dissolved organic matter in natural waters. *Limnol. Oceanogr.* **1994**, *39*, 1903–1916. [CrossRef]
28. Huguet, A.; Vacher, L.; Relexans, S.; Saubusse, S.; Froidefond, J.M.; Parlanti, E. Properties of fluorescent dissolved organic matter in the Gironde Estuary. *Org. Geochem.* **2009**, *40*, 706–719. [CrossRef]
29. Zsolnay, A.; Baigar, E.; Jimenez, M.; Steinweg, B.; Saccomandi, F. Differentiating with fluorescence spectroscopy the sources of dissolved organic matter in soils subjected to drying. *Chemosphere* **1999**, *38*, 45–50. [CrossRef]
30. Ohno, T. Fluorescence inner-filtering correction for determining the humification index of dissolved organic matter. *Environ. Sci. Technol.* **2002**, *36*, 742–746. [CrossRef]
31. Velapoldi, R.A.; Tønnesen, H.H. Corrected emission spectra and quantum yields for a series of fluorescent compounds in the visible spectral region. *J. Fluoresc.* **2004**, *14*, 465–472. [CrossRef]
32. Mueller, J.L.; Bidigare, R.R.; Trees, C.; Balch, W.M.; Dore, J.; Drapeau, D.T.; Karl, D.; Van Heukelem, L. *Ocean Optics Protocols for Satellite Ocean Color Sensor Validation, Revision 5. Volume V: Biogeochemical and Bio-Optical Measurements and Data Analysis Protocols*; Goddard Space Flight Space Center: Greenbelt, MD, USA, 2003.
33. Aeschbacher, M.; Sander, M.; Schwarzenbach, R.P. Novel electrochemical approach to assess the redox properties of humic substances. *Environ. Sci. Technol.* **2010**, *44*, 87–93. [CrossRef]
34. Aeschbacher, M.; Graf, C.; Schwarzenbach, R.P.; Sander, M. Antioxidant properties of humic substances. *Environ. Sci. Technol.* **2012**, *46*, 4916–4925. [CrossRef]
35. Paerl, R.W.; Claudio, I.M.; Shields, M.R.; Bianchi, T.S.; Osburn, C.L. Dityrosine formation via reactive oxygen consumption yields increasingly recalcitrant humic-like fluorescent organic matter in the ocean. *Limnol. Oceanogr. Lett.* **2020**. [CrossRef]
36. Min, D.W.; Kim, K.; Lui, K.H.; Kim, B.; Kim, S.; Cho, J.; Choi, W. Abiotic formation of humic-like substances through freezing-accelerated reaction of phenolic compounds and nitrite. *Environ. Sci. Technol.* **2019**, *53*, 7410–7418. [CrossRef]
37. Murphy, K.R.; Stedmon, C.A.; Wenig, P.; Bro, R. Open-Fluor–an online spectral library of auto-fluorescence by organic compounds in the environment. *Anal. Methods-UK* **2014**, *6*, 658–661. [CrossRef]
38. Harrison, A.F. The inhibitory effect of oak leaf litter tannins on the growth of fungi, in relation to litter decomposition. *Soil Biol. Biochem.* **1971**, *3*, 167–172. [CrossRef]